

Materials by numbers: Computations as tools of discovery

Uzi Landman[†]

School of Physics, Georgia Institute of Technology, Atlanta, GA 30332-0430

Edited by Bruce J. Berne, Columbia University, New York, NY, and approved March 24, 2005 (received for review January 21, 2005)

Current issues pertaining to theoretical simulations of materials, with a focus on systems of nanometer-scale dimensions, are discussed. The use of atomistic simulations as high-resolution numerical experiments, enabling and guiding formulation and testing of analytic theoretical descriptions, is demonstrated through studies of the generation and breakup of nanojets, which have led to the derivation of a stochastic hydrodynamic description. Subsequently, I illustrate the use of computations and simulations as tools of discovery, with examples that include the self-organized formation of nanowires, the surprising nanocatalytic activity of small aggregates of gold that, in the bulk form, is notorious for being chemically inert, and the emergence of rotating electron molecules in two-dimensional quantum dots. I conclude with a brief discussion of some key challenges in nanomaterials simulations.

nanocatalysis | nanoscience | nanowires | quantum dots | simulations of materials

To begin with, we comment on the origin of the first part of the title of this article, which is fashioned after the title of a 1988 News and Views column by Sir John Maddox (then the editor of *Nature*) (1). In that column, two papers (2, 3) describing the results of molecular dynamics (MD) simulations were highlighted: one in which the technique was applied to calculation of the dynamical properties of liquids (2), and one in which it was used for the first realistic treatment of the melting of a metal (aluminum) (3). Curiously, a similar theme is found in the third scene of Act I of Tom Stoppard's play *Arcadia* (4), where in Lady Thomasina Coverly, aged 13, states in the course of a conversation with her tutor: "God's truth, Septimus, if there is an equation for a curve like a bell, there must be an equation for one like a bluebell, and if a bluebell, why not a rose? Do we believe nature is written in numbers?" On another occasion, during a conversation about Newton's laws of motion and its impact on free will, Thomasina exclaims: "If you could stop every atom in its position and direction, and if your mind could comprehend all of the actions thus suspended, then if you were really good at algebra you could write the formula for all of the future; and although nobody can be so clever as to do it, the formula must exist just as if one could."

To put our discussion in a modern perspective, I recall here a famous statement made by P. M. Dirac in 1929 shortly after the introduction of the Schrödinger equation and its successful validation for simple systems like H₂ and He: "The fundamental laws necessary for the mathematical treatment of a large part of physics and the whole of chemistry are thus completely known, and the difficulty lies only in the fact that application of these laws leads to equations that are too complex to be

solved". During the second half of the last century, the usage of computers for investigations of basic and technological issues in the physical sciences and engineering (as well as in various other fields, including economy, finance, weather forecasting, and the health sciences) evolved and transformed from being aimed primarily at enabling and accelerating certain time-consuming numerical manipulations to their present status, where computer-based simulations serve as an indispensable powerful tool of discovery, supplementing and complementing (the more traditional) laboratory experiments and analytical theory as the pillars of scientific exploration. Indeed, methodological advances, novel algorithms, and innovative formulations of physical theories in forms that are amenable to numerical simulations, in symbiosis with the development and implementation of new computational platforms (for example, parallel and grid computing) and the innovative strides made in computer hardware over the last few decades, opened the door for investigations of systems and phenomena with ever-higher levels of complexity. These advances resulted in substantial progress and a number of remarkable discoveries.

To date, computer simulations have come of age, although outstanding challenges remain. Indeed, simulations of materials can provide information about complex materials phenomena under highly controllable conditions (that is, for a range of values of parameters characterizing the simulated system) and with refined resolution in space and time (that may exceed current experimentally attainable resolution limits). Such simulations allow researchers to gain understanding and deep insights into the microscopic physical and chemical origins of materials behavior. The knowledge thus acquired is often used for the interpretation and elucidation of

experimental observations, as guidance for the planning of future experiments, and in the design of technological devices. Moreover, in certain occasions, a simulation may be the preferred, and sometimes the only, interrogation method; such is the case with systems that may be difficult or impossible to prepare (although their existence is consistent with known physical laws, and when there is other evidence for their occurrence, e.g., astronomical or geophysical observations), systems that may be hazardous under normal laboratory conditions, systems under extreme conditions that may be impractical or undesirable to attempt in the laboratory, and situations where laboratory experiments are prohibited by environmental, societal, or political reasons (such as experimentation on nuclear waste and the nuclear stockpile).

Computer simulations are sometimes likened to numerical experiments because they allow interrogation of the consequences that arise from controlled variation of the simulated model, as well as their "brute force" nature; that is, generating (with minimal approximations) numerical solutions to the equations (classical, quantum, or hybrids of the two) that describe the evolution of the system. This methodology results in certain advantages, including the ability to study many-particle systems (i.e., a large number of degrees of freedom) characterized by complex interactions without the employment of "coarse graining," linearization (of the interpar-

This paper was submitted directly (Track II) to the PNAS office.

Abbreviations: MD, molecular dynamics; LE, lubrication equation; SLE, stochastic LE; QD, quantum dot; sS, spin-and-space; UHF, unrestricted Hartree-Fock; CPD, conditional probability distribution; RWM, rotating Wigner molecule; QM, quantum mechanics; MM, molecular mechanics.

[†]E-mail: uzi.landman@physics.gatech.edu.

© 2005 by The National Academy of Sciences of the USA

ticle interactions or of response characteristics), and other simplifying assumptions. This “noncompromising” nature of computer-based simulations, applied to well posed models, endows them with the ability to unveil, in certain cases, new, emergent (5) behavior that may be regarded as arising from a higher level of organization and complexity than that which may be predicted, or explained (through common methods of analysis), from the primary simulation model or found through the use of simplified analytical approximations. Furthermore, such theoretical experiments, when used with adherence to strict standards pertaining to the range of validity and faithfulness of the simulated model, can serve as numerical microscopies of reliable descriptive and predictive power. Moreover, in certain circumstances, the results of a computer simulation may serve as theoretically generated data (i.e., as a substitute to laboratory recorded results when such are lacking), which may be used as the basis for the formulation, development, and testing of analytical theories.

Small Is Different: Physical and Chemical Phenomena in Nanoscale Systems

Characterization and elucidation of size-dependent patterns of the properties of finite materials’ aggregates exhibiting discrete quantized energy level spectra and specific structures and morphologies, investigations of the unique properties of finite-size materials clusters, and studies of the nature of the evolution of materials’ properties from the molecular and cluster regimes to the bulk phase are among the major challenges of modern materials science, and as such, these issues have been the subject of intensive research endeavors.

In many instances, it has been found that, for larger materials’ aggregates, the deviation of the properties from the bulk limit scales with the size of the aggregate. However, in many cases, at sufficiently small sizes (often in the nanoscale regime), the dependence of the material property on size becomes non-scalable; at this point, small is different in an essential way, with the physical and chemical properties becoming emergent in nature, i.e., they can no longer be deduced from those known for larger sizes (6–10).

In most cases, when the non-scalable regime is approached, the physical size of the system along at least one of the coordinate axes becomes comparable to a phenomenon-dependent characteristic length; examples include: conductance quantization occurring when the diameter of the constriction (e.g., a nanowire) approaches the electronic Fermi-wave-

length (typically 0.5 nm in metals), i.e., “when the electron feels the boundary”; transport in a wire becoming ballistic (rather than diffusive) when the length of the wire is shorter than the electron mean-free-path (11); a column (or a jet) of inviscid fluid becoming unstable when its length equals approximately nine times its radius (this length equals the wavelength of the fastest growing varicose instability mode, known as the Rayleigh instability; ref. 12); and the mechanical response and deformation modes of nanocrystals becoming dislocationless when their physical dimensions are comparable to the dislocation core size, resulting in enhanced mechanical strength of nanoscale crystallites and nanowires (13, 14), as well as mechanical reversibility (14) and absence of work-hardening.

Here, I highlight certain developments in areas pertaining to physical and chemical materials phenomena, focusing on theoretical simulations of systems with nanometer dimensions. This article is not intended as a review. Instead, I summarize my experience and view point on the subject, and use examples from my own work as illustrations; however, this does not imply in any way that other appropriate examples cannot be found.

Case Studies: New Behavior, Surprises, and Emergent Phenomena Revealed Through Simulations

The eternal mystery of the world is its comprehensibility. The fact that it is comprehensible is a miracle.

Albert Einstein

Formation and Breakup of Nanojets: The Use of Simulations as Theoretical Experiments. Liquid jets of macroscopic dimensions and their breakup into drops have been the subject of active scientific (12, 15, 16), as well as technological, interest. As the transverse length-scale (i.e., diameter) of the jet approaches the molecular scale, the validity of commonly used continuum fluid dynamics treatments, including Rayleigh’s (12) original linear stability analysis of inviscid fluids and its extensions (15), as well as computational fluid dynamical simulations of the Navier–Stokes equations and treatments based on the so-called lubrication equation (LE) (sometimes called the “slenderness approximation,” ref. 15) in which averaging over the lateral cross-section of the jet is performed, become questionable (16, 17). In particular, because of the reduced dimensions, the behavior of such systems involves large spatio-temporal variations and fluctuations of the liquid properties

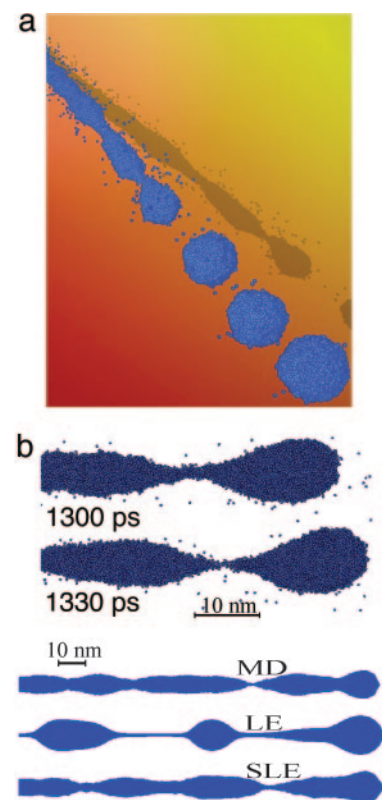


Fig. 1. Atomistic and continuum nanojet configurations. (a and b Upper) Atomistic configurations obtained with MD simulations of a propane nanojets emanating from a 6-nm diameter nozzle, illustrating the development of instabilities and a double-cone pinch-off configuration. Each small blue sphere represents a propane molecule. (b Lower) An atomistic MD configuration (double-cone break-up) (Top), a configuration resulting from solution of the deterministic lubrication equation (LE) exhibiting a long thread, in disagreement with the MD data (Middle), and the solution of the stochastic LE (SLE) showing agreement with the MD simulation (Bottom). This figure was modeled after ref. 16.

(such as temperature gradients and liquid density changes caused by viscous heating and evaporative cooling), requiring the development of physically reliable and accurate atomistic-scale simulations. In light of these considerations, the first issue that needs to be resolved pertains to the very existence and stability of contiguous elongated liquid structures (e.g., liquid bridges or jets) of nanometer dimensions.

Results from MD simulations (16), performed for a common fuel (propane, C_3H_8) as a fluid confined and injected into vacuum through a nozzle of 6 nm diameter, are shown in Figs. 1 and 2. Generation of the nanojet required the application of a back pressure of 500 MPa, with the exterior surface of the gold nozzle heated to the boiling temperature of propane (230 K) to prevent condensation of thick blocking films

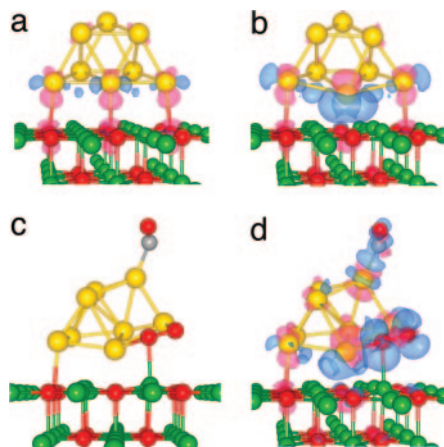


Fig. 5. Cluster configurations and charging. (a and b) Charge-difference isosurfaces for an Au_8 cluster when adsorbed on a perfect MgO (001) surface (a) and when anchored to a surface F-center, i.e., $Au_8/MgO(FC)$ (b). Au atoms are shown in yellow, O atoms are shown in red, and Mg atoms are shown in green. Note the significantly enhanced degree of charge transfer to the Au_8 in b. (c) The optimal configuration of the reaction complex $Au_8/O_2/CO/MgO(FC)$, a surface-supported gold octamer with an interfacially adsorbed O_2 molecule and a CO adsorbed on the top triangular facet. Note the significant change in the geometry of the Au_8 in comparison with the bare cluster displayed in a, illustrating the structural fluxionality of small clusters. The C atom is depicted in gray. (d) Isosurfaces of the charge difference between the reaction complex (see c) and the isolated components, illustrating excess electronic charge localization on the adsorbed reactant molecules. Pink isosurfaces represent $\delta\rho < 0$ (depletion), and blue isosurfaces correspond to $\delta\rho > 0$ (excess). All of the isosurfaces are plotted for the same (absolute) value of the density difference ($\delta\rho$) to allow direct comparison between the different cases. This figure was modeled after ref. 46.

caused by chemical contamination (see also a recent discussion of the interaction of hydrogen with gold nanowires; ref. 60).

Gold Nanocatalysis. Unlike supported particles of larger size or extended solid surfaces (61), small metal clusters adsorbed on support materials were found to exhibit unique properties that originate from the highly reduced dimensions of the individual metal aggregates (32, 38–46). In particular, investigations on size-selected small gold clusters, Au_n ($20 \geq n \geq 2$), soft-landed (62) on a well characterized metal-oxide support [specifically, a MgO (001) surface, with and without oxygen vacancies, or F-centers], revealed (40) that gold octamer (Au_8) clusters bound to F-centers of the magnesia surface are the smallest known gold heterogeneous catalysts that can oxidize CO into CO_2 at temperatures as low as 140 K. The same cluster adsorbed on a MgO surface without oxy-

gen vacancies is catalytically inactive for CO combustion (40).

Quantum mechanical *ab initio* simulations (including scalar relativistic corrections; refs. 63 and 64), in juxtaposition with laboratory experiments, led us to conclude (40, 43, 46) that the key for low-temperature gold catalysis in CO oxidation is the binding of O_2 and CO to the supported gold nanocluster, which activates the O—O bond to a peroxo-like (or superoxo-like) adsorbate state. Charging of the metal cluster, caused by partial electron transfer from the substrate F-center into the deposited cluster (see Fig. 5), underlies the catalytic activity of the gold octamers (Au_8), as well as that of other small gold clusters (Au_n , $8 \leq n \leq 20$). These investigations predicted that (i) oxygen vacancy (F-centers) on the metal-oxide support surface play the role of “active-sites” (a concept that has been central to the development of heterogeneous catalysis); (ii) these sites serve to anchor the deposited clusters more strongly [binding energy, $E_B = 3.44$ eV for Au_8 to $MgO(FC)$] than sites on the undefective surface ($E_B = 1.22$ eV), thus inhibiting their migration and coalescence; and most importantly, (iii) these active sites control the charge-state of the gold clusters, thus promoting the activation of adsorbed reactant molecules (i.e., formation of the aforementioned peroxo or superoxo species; refs. 40, 43, and 46).

The correlation diagram in Fig. 6 shows that the local density of states projected on the adsorbed oxygen molecule in the reaction complex overlaps with the entire d-band of the Au_8 clus-

ter (see Fig. 6 *Center* in the range of -10 eV $\leq E \leq E_F$, where E_F is the Fermi energy). The antibonding $2\pi^*$ states of O_2 are pulled below E_F , and thus the full spin manifold of these states is populated in the reaction complex (resulting in the aforementioned partial excess charge on the adsorbed molecule). The occupation of the antibonding level results in strong weakening (activation) of the O—O bond that is reflected in a significant increase of its length (1.43 Å, compared to that of the free oxygen molecule, 1.25 Å). Accompanying the activation process is a change in the spin state of the molecule from a triplet state in the gas phase to a peroxo-like adsorbed state with a zero net spin.

A different scenario is found for smaller gold clusters, as well as for gold clusters adsorbed on a perfect magnesia surface (that is, with no F-centers). In these cases, we find a smaller projected density of states on the adsorbed gold cluster near E_F , leading to a weaker (or no) resonance with the antibonding orbitals of the adsorbed reactant molecules, thus resulting in weak binding of the molecule to the cluster with a consequent small degree of activation and reduced chemical reactivity; these results have indeed been observed experimentally under these situations.

Symmetry Breaking in Quantum Dots (QDs): Electron Molecules. Two-dimensional QDs, created at semiconductor interfaces through the use of lithographic and gate-voltage techniques, with refined control of their size, shape, and

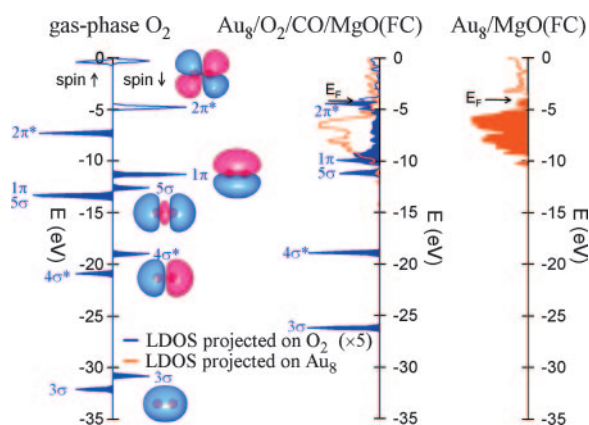


Fig. 6. A correlation diagram depicting the local density of states (LDOS) for a gas-phase O_2 molecule (Left), the bare gold octamer adsorbed on the F-center defect ($Au_8/MgO(FC)$ (Right)), and for the reaction complex with the adsorbed reactant molecules, $Au_8/O_2/CO/MgO(FC)$ (Center). The LDOS is projected on the adsorbed gold cluster. (Center) The LDOS projected on the peripherally adsorbed O_2 as well as on the gold octamer. (Left) Images of the orbitals of the free O_2 molecule. LDOS projected on O_2 is depicted in blue, and on LDOS projected on gold is depicted in orange. Filled (empty) features correspond to occupied (unoccupied) orbitals. (Center) The region in blue overlapping the density of states of gold corresponds mainly to occupation of the 1π and $2\pi^*$ orbitals of the adsorbed molecule. This figure was modeled after ref. 46.

number of electrons, are often referred to as “artificial atoms” (65, 66). These systems are expected, with the use of applied magnetic fields, to have future applications as logic gates in quantum computing and as nanoscale switching devices. As indicated above, certain analogies have been made between these man-made systems and their natural counterparts, suggesting that the physical nature of electrons in the former is similar to that underlying the traditional description of natural atoms, pertaining particularly to electronic shells and the Aufbau principle in atoms (where electrons are taken to be moving in a spherically averaged effective central mean-field potential).

The above analogy has been challenged recently (67, 68) on the basis of calculations that showed evidence for formation (under conditions that are readily achieved in the laboratory) of “electron molecules,” which are alternatively called Wigner molecules after the physicist who predicted formation of electron crystals in extended systems (69). The mean-field spin-and-space (sS) unrestricted Hartree–Fock (UHF) calculations used here (denoted as sS-UHF) for electrons confined by a parabolic potential in 2D QDs led to the discovery of spontaneous symmetry breaking (that is, the spontaneous reduction in the symmetry of a system that is driven by the stability thus acquired; ref. 6), manifested by the appearance of spatial interelectronic (crystalline) correlations (even in the absence of magnetic fields).

Symmetry breaking (at the mean-field level of the calculation, see below) may indeed be expected, based on the interplay between the interelectron repulsion, Q , and the zero-point kinetic energy, K . Taking $Q = e^2/\kappa l_0$ and $K \equiv \hbar \omega_0$ [where $l_0 = (\hbar/m^* \omega_0)^{1/2}$ is the spatial extent of an electron in the lowest state of the parabolic confinement; m^* is the electron effective mass, κ is the dielectric constant, and ω_0 is the frequency that characterizes the parabolic confining potential], the Wigner parameter is defined as $R_W = Q/K$. Symmetry breaking may be expected when the interelectron repulsion dominates, i.e., for $R_W \geq 1$. Under such circumstances, an appropriate approximate (mean-field) solution of the Schrödinger equation necessitates consideration of wave functions with symmetries that are lower than that of the circularly symmetric QD Hamiltonian. Such solutions may be found through the use of the sS-UHF method, where all restrictions on the symmetries of the wave functions, as well as the double occupancy requirement (which is inherent to the restricted HF, i.e. RHF, method) are lifted. From the above, we

note that the state of the system may be controlled and varied through the choice of materials (i.e., κ) and/or the strength of the confinement (ω_0), because $R_W \propto 1/(\kappa \sqrt{\omega_0})$.

Formation of “electron molecules” has been investigated through exact calculations for two-electron confined parabolically in a QDs (70); for exact diagonalization of the Hamiltonian for three electrons in a parabolic QD with $B = 0$, see ref. 71. For the two electron case, the terms in the Hamiltonian corresponding to the center-of-mass and the interelectron relative degrees of freedom are separable. The spectrum obtained for large values of R_W exhibits features that are characteristic of a collective rovibrational dynamics, akin to that of a natural “rigid” triatomic molecule with an infinitely heavy middle particle representing the center of mass of the dot (see Fig. 9, which is published as supporting information on the PNAS web site). This spectrum transforms to that of a “floppy” molecule for smaller value of R_W (i.e., for stronger confinements characterized by a larger value of ω_0 , and/or for weaker interelectron repulsion), ultimately converging to the independent-particle picture with the circular central mean-field of the QD. Further evidence for the formation of the electron molecule was found through examination of the conditional probability distribution (CPD), $P(\mathbf{r}, \mathbf{r}_0)$, which expresses the probability of finding a particle at \mathbf{r} given that the “observer” (reference point) is riding on another particle at \mathbf{r}_0 (68, 70).

The general 2D Hamiltonian of the system describes N electrons interacting by a Coulomb repulsion, confined by a circular parabolic potential of frequency ω_0 and subjected to a perpendicular magnetic field \mathbf{B} . The solutions to the Schrödinger equation must have good angular momentum, L , and spin quantum numbers (the latter is guaranteed in the fully spin-polarized, high B , case). As described in detail (72–77), these solutions can be well approximated by a two-step method, with symmetry breaking occurring in the first step (at the sS-UHF level), followed by a second step where symmetry is restored by projection techniques.

We note here that the broken symmetry states obtained through the sS-UHF method are lower in energy than the UHF solutions, with further lowering of the energy resulting from application of the symmetry-restoring spin and angular momentum projections (76). By definition, these energy lowerings with respect to the RHF energy correspond to gain of electron correlation energy (see Fig. 10, which is published as supporting in-

formation on the PNAS web site). An angular-momentum-projected state is called a “rotating Wigner molecule” (RWM). The electron-molecule structure of these states is revealed through analysis of their conditional probability distribution.

To illustrate the emergence of RWM in parabolically confined QDs under high B (79), Fig. 7 shows results obtained (75) through the aforementioned two-step computational technique for $N = 7, 8$, and 9 electrons, and compare them with the results derived from exact diagonalization of the Hamiltonian. Systematic investigations of QDs under variable magnetic fields revealed ground electronic states of crystalline character. These states are found for particular “magic” angular momentum values (L) that exhibit enhanced stability, called cusp states. For a given value of B , one of these L s corresponds to the global minimum, i.e., the ground state, and varying B causes the ground state and its angular momentum to change. The cusp states have been long recognized (80) as the finite- N precursors of the fractional quantum Hall effect states in extended systems. In particular, the fractional fillings ν (defined in the thermodynamic limit) are related to the magic angular momenta of the finite- N system as (81), $\nu = N(N - 1)/2L$.

Recently derived parameter-free wave functions corresponding to the RWM picture in QDs, characterized by prominent crystalline correlations, have been shown to provide a simple, improved, and consistent description of the cusp states, superior to the liquid-like characteristics obtained through wave functions developed in the context of the fractional quantum Hall effect (82, 83) (particularly for high angular momenta, corresponding to low fractional fillings ν ; refs. 72 and 73). The ground-state crystalline arrangements of the electron (Wigner) molecules were found (72–75) to consist of concentric polygonal rings rotating independently of each other (see in particular the CPDs for the two rings shown for $N = 9$ in Fig. 7), with the electrons on each ring rotating coherently (75). The rotations stabilize the RWM relative to the static one; namely, the projected (symmetry-restored) states (that are multideterminantal) are lower in energy compared to the broken-symmetry ones (the single determinantal sS-UHF solutions).

Formation of electron molecules is enhanced for nonspherical confining potentials (76). Indeed, evidence for formation of a two-electron molecule has been inferred most recently from transport measurements on elliptical 2D

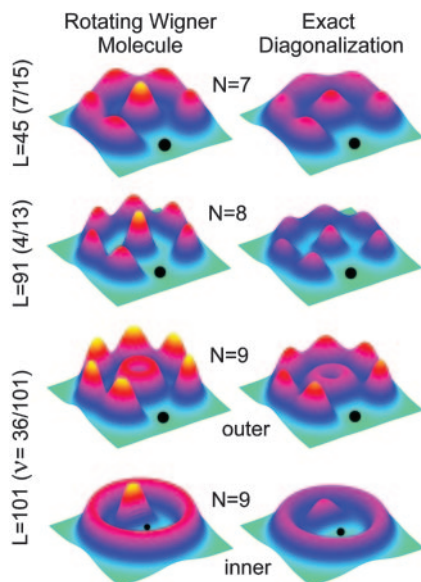


Fig. 7. CPDs at high B, evaluated for parabolic quantum dots through (i) the two-step procedure of symmetry breaking and subsequent restoration, resulting in RWM (Left), and (ii) exact diagonalization (Right). The angular momentum values and corresponding values of the fractional filling are given on the left. The optimal polygonal structure for a given N is given by (n_1, n_2) with $n_1 + n_2 = N$. For $N = 7, 8$, and 9 , these arrangements are $(1, 6)$, $(1, 7)$, and $(2, 7)$, respectively. The reference point for the calculation of the CPD is denoted by a filled dot. Note in particular the two CPDs shown for $n = 9$, illustrating that, for a reference point located on the outer ring, the inner ring appears uniform, and vice versa for a reference point located on the inner ring (Bottom). These results illustrate that the rings rotate independently of each other. This figure was modeled after ref. 75.

QDs (84), and these systems have also been addressed theoretically (85).

The emergence of crystalline geometric arrangements, discussed above for electrons confined in 2D quantum dots, appears to be a general phenomenon that is predicted (86) to occur also for trapped bosonic atomic systems (neutral or charged) when the interatomic repulsion is tuned to exceed the characteristic energy of the parabolic potential of the trap. These highly correlated trapped 2D states exhibit localization of the bosons into polygonal-ring-like crystalline patterns, and thus extend to higher dimensions earlier work that predicted localization of strongly repelling 1D bosons, often referred to as the Tonk-Girardeau regime (see ref. 86 and references therein to pertinent theoretical and recent experimental observations).

Challenges: Extending Spatial and Temporal Scales

If God created the world, his primary concern was certainly not to make its understanding easy for us

Albert Einstein

Among the many challenges facing computational investigations of materials, I selected here certain issues that arise when attempting to extend the spatial dimensions and time intervals of dynamical simulations of materials.

Many of the research activities involving materials systems of highly reduced (nanoscale) dimensions are focused on identification and elucidation of the unique behavior of materials in the non-scalable size regime. Stated in an alternative fashion, investigations of nanoscale materials respond to the quest to identify and understand size-dependent patterns that underlie the evolution of materials' properties, starting from the atomic and molecular regime, proceeding to small clusters, nanoscale aggregates, and mesoscopic materials, and ultimately arriving to the bulk condensed phase domain. The search for size-evolutionary patterns requires the development of an arsenal of theoretical methodologies and techniques appropriate for treating materials systems with varying sizes and dimensionalities.

Common to the above issues is the need to extend the simulations to larger systems. Methodologies that aim at this goal (although direct MD simulations, i.e., direct integration of Newton's equations of motion for a system consisting of multimillion interacting particles, are possible; refs. 87 and 88) are commonly referred to as multiscale modeling methods, and they include (i) procedures for embedding atomistic regions in continuum environments (such as in treatments of mechanical properties and response of materials, indentation, fracture, crack initiation and propagation, and film growth processes) (89, 90) and (ii) methods for embedding of regions that are treated quantum mechanically (QM) in environments that are treated classically (with atomic resolution) (91, 92); the latter embedding scheme is often referred to as QM/MM, where MM stands for molecular mechanics, although the MD method is used in most modern applications. We note that, in recent years, efforts have been invested also in combining the entire multiscale spectrum (classical continuum, classical atomistic, and QM) into a single simulation (90).

The key to the success of embedding schemes is the formulation and implementation of "seamless" interfaces that couple the various regions (e.g., QM, classical-atomistic, and continuum). As an illustration of the results of a QM/MM simulation, Fig. 8 shows results for the ionization hole in DNA (93) taken from a most recent investigation of the reaction of water with ion-

ized DNA (R. N. Barnett, A. Bongiorno, C. L. Cleveland, A. Joy, U.L., and G. B. Schuster, unpublished data, and refs. 94 and 95). For other recent studies employing the QM/MM methodology, see refs. 96 and 97.

An alternative approach to the simulation size problem is offered by coarse-grain models, reviewed recently in ref. 98. In these methods, which have found

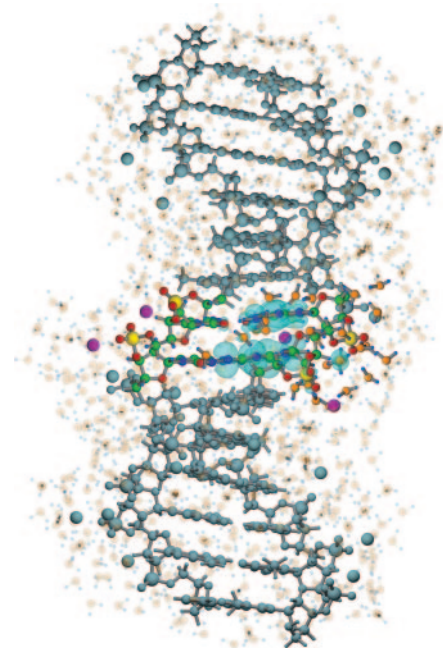


Fig. 8. QM/MM calculation of the ionization hole in a 14-bp oligomer of B-DNA d(5'-AAGGAAG-GAAGGAA-3'), where the bold letters denote the region treated quantum mechanically (QM). The atoms in the QM region are shown in color, and those in the classical MM region are depicted in blue-gray; the classically treated H₂O molecules are depicted as a background shadow. The hole density (electron density difference between the neutral and ionized system, both calculated for the same geometry) is superimposed on the QM region, and it appears as the light blue iso-surfaces localized on the GG doublet. There are 3,105 atoms in the MM region (12 base pairs, 775 water molecules, and 22 Na ions), and the QM region contains 221 atoms [two base pairs (G—C)₂ linked by sugar-phosphate groups, 29 water molecules, and four Na atoms]. A total of 680 valence electrons were included in the QM calculation. In the QM region, the color assignments are as follows: P, yellow; C, green; N, blue; O (base), red; O (phosphate), red; O (H₂O), orange; H (H₂O), small blue spheres; Na, purple. Note that most of the counterions are located in the vicinity of the phosphate groups, with one of the counterions in the QM region residing in the major groove. The QM/MM method used here was developed by A. Bongiorno, S. B. Suh, R. N. Barnett, and U.L. (unpublished data). The QM calculations were performed by using the method described in ref. 54, with generalized gradient corrections (GGA) (94) and a plane-wave basis with a 62Ry kinetic-energy cutoff. In the classical (MM) region, the AMBER 96 potentials (95) were used.

applications mainly in soft-matter simulations, a coarsened model of the simulated system is constructed and parametrized, with coarse-grained particles (“superatoms”) representing groups of (real) atoms or whole molecular segments.

Another set of challenges arise in connection with the time-scale gap; i.e., issues pertaining to limitations in the accessible simulation time intervals for which the dynamical evolution of materials systems may be simulated. Of particular interest are systems and processes that are characterized by the presence of different relevant time scales (a chemical reaction where the reaction time may be larger by orders of

magnitude than the period of molecular vibrational is an example of a system with a separation of time scales). Issues pertaining to limitations of the time scales accessible to dynamic simulations remain serious problems that are not likely to be solved (merely) by progress in computational hardware because of the sequential (time-step-by-time-step) nature of the solution of the classical equations of motion. Currently, the methods that have been proposed for “boosting” the simulated time span address, mainly, processes characterized by infrequent events (e.g., bulk and surface diffusion of atoms or clusters; ref. 99).

I am indebted to all of my colleagues who made invaluable contributions to the research

described in this article. In particular, I note those whose work I used in this article: Robert N. Barnett, Eduard Bogachek, Angelo Bongiorno, Charles L. Cleveland, Jianping Gao, Hannu Hakkinen, Ueli Heiz, W. David Luedtke, Michael Moseler, Andrew Scherbakov, Gary B. Schuster, Constantine Yannouleas, and Bokwon Yoon. The research described in this article was supported over the years by the U.S. Air Force Office of Scientific Research, the U.S. Department of Energy, and the National Science Foundation. The calculations were performed at the National Energy Research Scientific Computing Center at the Lawrence Berkeley National Laboratory, on the U.S. Department of Defense Computers supported by the High Performance Computing Modernization Program, and at the Georgia Institute of Technology Center for Computational Materials Science.

- Maddox, J. (1988) *Nature* **334**, 561.
- Colvin, M. E., Ladd, A. J. C. & Alder, H. J. (1988) *Phys. Rev. Lett.* **61**, 381–384.
- Stolze, P., Norskov, J. K. & Landman, U. (1988) *Phys. Rev. Lett.* **61**, 440–443.
- Stoppard, T. (1993) *Arcadia* (Faber and Faber, London).
- Batterman, R. W. (2002) *The Devil in the Details* (Oxford Univ. Press, Oxford).
- Landman, U., Barnett, R. N., Moseler, M. & Yannouleas, C. (2001) *The Physics and Chemistry of Clusters, Proceedings of the Nobel Symposium 11*, eds. Campbell, E. E. B. & Larsson, M. (World Scientific, Singapore), pp. 42–68.
- Landman, U. (1998) *Solid State Comm.* **107**, 693–708.
- Bhushan, B., Israelachvili, J. N. & Landman, U. (1995) *Nature* **374**, 607–616.
- Landman, U., Luedtke, W. D. & Gao, J. (1996) *Langmuir* **12**, 4514–4528.
- Landman, U. & Luedtke, W. D. (2004) *Faraday Dis.* **125**, 1–22.
- Landauer, R. (1970) *Philos. Mag.* **21**, 863–873.
- Rayleigh, J. W. S. (1879) *Proc. R. Soc. London* **10**, 4–13.
- Landman, U., Luedtke, W. D., Burnham, N. A. & Colton, R. J. (1990) *Science* **248**, 454–461.
- Landman, U., Luedtke, W. D., Salisbury, B. E. & Whetten, R. L. (1996) *Phys. Rev. Lett.* **77**, 1362–1365.
- Eggers, J. (1997) *Rev. Mod. Phys.* **69**, 865–930.
- Moseler, M. & Landman, U. (2000) *Science* **289**, 1165–1169.
- Shi, X. D., Brenner, M. P. & Nagel, S. R. (1994) *Science* **265**, 219–222.
- Landau, L. D. & Lifshitz, E. M. (1984) *Fluid Mechanics* (Pergamon, Oxford).
- Eggers, J. (2002) *Phys. Rev. Lett.* **89**, 084502.
- de Heer, W. A. (1993) *Rev. Mod. Phys.* **65**, 611–675.
- Yannouleas, C. & Landman, U. (1996) in *Large Clusters of Atoms and Molecules*, NATO ASI Series E, ed. Martin, T. P. (Kluwer, Dordrecht, The Netherlands), Vol. 313, pp. 131–200.
- Yannouleas, C., Landman, U. & Barnett, R. N. (1999) in *Metal Clusters*, ed. Ekardt, W. (Wiley, New York) pp. 145–180.
- Yannouleas, C. & Landman, U. (1997) *J. Phys. Chem. B* **101**, 5780–5783.
- Stafford, C. A., Baeriswyl, D. & Burki, J. (1997) *Phys. Rev. Lett.* **79**, 2863–2866.
- Yannouleas, C., Bogachek, E. N. & Landman, U. (1998) *Phys. Rev. B* **57**, 4872–4882.
- Whetten, R. L., Khoury, J. T., Alvarez, M., Murthy, S., Vezmar, I., Wang, Z. L., Stephens, P. W., Cleveland, C. L., Luedtke, W. D. & Landman, U. (1996) *Adv. Mater.* **8**, 428–433.
- Luedtke, W. D. & Landman, U. (1996) *J. Phys. Chem. B* **100**, 13323–13329.
- Hakkinen, H., Barnett, R. N. & Landman, U. (1999) *Phys. Rev. Lett.* **82**, 3264–3267.
- Collier, C. P., Vossmeier, T. & Heath, J. R. (1998) *Annu. Rev. Phys. Chem.* **49**, 371–404.
- Whitesides, G. M. & Crzykowski, B. (2002) *Science* **295**, 2418–2421.
- Billas, I. M. L., Chatelain, A. & deHeer, W. A. (1994) *Science* **265**, 1682–1684.
- Moseler, M., Hakkinen, H., Barnett, R. N. & Landman, U. (2001) *Phys. Rev. Lett.* **86**, 2545–2548.
- Moseler, M., Hakkinen, H. & Landman, U. (2002) *Phys. Rev. Lett.* **89**, 176103.
- Yannouleas, C., Barnett, R. N. & Landman, U. (1995) *Commun. At. Mol. Phys.* **31**, 445–460.
- Barnett, R. N., Landman, U. & Rajagopal, G. (1991) *Phys. Rev. Lett.* **67**, 3058–3061.
- Brechignac, C., Cahuzac, P., Carlier, F., de Frutos, M., Barnett, R. N. & Landman, U. (1994) *Phys. Rev. Lett.* **72**, 1636–1639.
- Yannouleas, C., Landman, U., Hertlet, A. & Schweikhard, L. (2001) *Phys. Rev. Lett.* **86**, 2996–2999.
- Haruta, M. (1997) *Catal. Today* **36**, 153–166.
- Valden, M., Lai, X. & Goodman, D. W. (1998) *Science* **281**, 1647–1650.
- Sanchez, A., Abbet, S., Heiz, U., Schneider, W.-D., Hakkinen, H., Barnett, R. N. & Landman, U. (1999) *J. Phys. Chem. A* **103**, 9573–9578.
- Hakkinen, H. & Landman, U. (2001) *J. Am. Chem. Soc.* **123**, 9704–9705.
- Soaciu, L. D., Hagen, J., Bernhardt, T. M., Wöste, L., Heiz, U., Hakkinen, H. & Landman, U. (2003) *J. Am. Chem. Soc.* **125**, 10437–10445.
- Hakkinen, H., Abbet, S., Sanchez, A., Heiz, U. & Landman, U. (2003) *Angew. Chem. Int. Ed.* **42**, 1297–1300.
- Yoon, B., Hakkinen, H. & Landman, U. (2003) *J. Phys. Chem. A* **107**, 4066–4071.
- Cho, A. (2003) *Science* **299**, 1684–1685.
- Yoon, B., Hakkinen, H., Landman, U., Worz, A. S., Antonietti, J. M., Abbet, S., Judai, K. & Heiz, U. (2005) *Science* **307**, 403–407.
- Pascual, J. I., Mendez, J., Gomez-Herrero, J., Baro, A. M., Garcia, N., Landman, U., Luedtke, W. D., Bogachek, E. N. & Cheng, H.-P. (1995) *Science* **267**, 1793–1795.
- Rubio, G., Agraït, N. & Vieira, S. (1996) *Phys. Rev. Lett.* **76**, 2302–2305.
- Agraït, N., Levi-Yeyati, A. & van Ruitenbeek, J. M. (2003) *Phys. Rep.* **377**, 81–279.
- Gao, J., Luedtke, W. D., Gourdon, D., Ruths M., Israelachvili, J. N. & Landman, U. (2004) *J. Phys. Chem. B* **108**, 3410–3425.
- Stalder, A. & Durig, U. (1996) *Appl. Phys. Lett.* **68**, 637–639.
- Gimzewski, J. K., Moller, R., Pohl, D. W. & Schlittler, R. R. (1987) *Surface Sci.* **189/190**, 15–23.
- Eigler, D. M., Lutz, C. P. & Rudge, W. E. (1991) *Nature* **352**, 600–603.
- Barnett, R. N. & Landman, U. (1993) *Phys. Rev. B* **48**, 2081–2097.
- Barnett, R. N. & Landman, U. (1997) *Nature* **387**, 788–791.
- Ohnishi, H., Kondo, Y. & Takayanagi, K. (1998) *Nature* **395**, 780–783.
- Rodrigues, V. & Ugarte, D. (2001) *Phys. Rev. B* **63**, 073405.
- Hakkinen, H., Barnett, R. N., Scherbakov, A. G. & Landman, U. (2000) *J. Phys. Chem. B* **104**, 9063–9066.
- Hakkinen, H., Barnett, R. N. & Landman, U. (1999) *J. Phys. Chem. B* **103**, 8814–8816.
- Barnett, R. N., Hakkinen, H., Scherbakov, A. G. & Landman, U. (2004) *Nano Lett.* **4**, 1845–1852.
- Ertl, G. & Freund, H.-J. (1999) *Phys. Today* **52**, 32–38.
- Cheng, H.-P. & Landman, U. (1993) *Science* **260**, 1304–1307.
- Hakkinen, H., Moseler, M. & Landman, U. (2002) *Phys. Rev. Lett.* **89**, 033401.
- Hakkinen, H., Yoon, B., Landman, U., Li, X., Zhai, H.-J. & Wang, L.-S. (2003) *J. Phys. Chem.* **107**, 6168–6175.
- Kastner, M. A. (1993) *Phys. Today* **46**, 24–27.
- Tarucha, S., Austing, D. G., Honda, T., van der Hage, R. J. & Kouwenhoven, L. P. (1996) *Phys. Rev. Lett.* **77**, 3613–3616.
- Yannouleas, C. & Landman, U. (1999) *Phys. Rev. Lett.* **82**, 5325–5328; and erratum (2000) **85**, 2220.
- Yannouleas, C. & Landman, U. (2000) *Phys. Rev. B* **61**, 15895–15904.
- Wigner, E. (1934) *Phys. Rev.* **46**, 1002–1011.
- Yannouleas, C. & Landman, U. (2000) *Phys. Rev. Lett.* **85**, 1726–1729.
- Mikhailov, S. A. (2002) *Phys. Rev. B* **65**, 115312.
- Yannouleas, C. & Landman, U. (2002) *Phys. Rev. B* **66**, 115315.
- Yannouleas, C. & Landman, U. (2003) *Phys. Rev. B* **68**, 035325.
- Yannouleas, C. & Landman, U. (2004) *Phys. Rev. B* **69**, 113306.
- Yannouleas, C. & Landman, U. (2004) *Phys. Rev. B* **70**, 235319.
- Yannouleas, C. & Landman, U. (2002) *Int. J. Quant. Chem.* **90**, 699–708.
- Yannouleas, C. & Landman, U. (2002) *J. Phys. Condens. Matter* **14**, L591–L598.
- Luedtke, W. D. & Landman, U. (1991) *J. Vac. Sci. Technol. B* **9**, 414–421.
- Maksym, P. A. (1996) *Phys. Rev. B* **53**, 10871–10886.
- Laughlin, R. B. (1983) *Phys. Rev. B* **27**, 3383–3389.
- Girvin, S. M. & Jach, T. (1983) *Phys. Rev. B* **28**, 4506–4509.
- Laughlin, R. B. (1987) in *The Quantum Hall Effect*, eds. Prange, R. E. & Girvin, S. M. (Springer, New York), p. 233.
- Mandal, S. S., Peterson, M. R. & Jain, J. K. (2003) *Phys. Rev. Lett.* **90**, 106403.
- Zumbuhl, D. M., Marcus, C. M., Hanson, M. P. & Gossard, A. C. (2004) *Phys. Rev. Lett.* **93**, 256801–1–256801–4.
- Yannouleas, Y. & Landman, U. (2005) arXiv:cond-mat/0501612.
- Romanovsky, I., Yannouleas, C. & Landman, U. (2004) *Phys. Rev. Lett.* **93**, 230405.
- Abraham, F. F. (2003) *Adv. Phys.* **52**, 727–790.
- Kodiyalam, S., Kalia, R. K., Nakano, A. & Vashishta, P. (2004) *Phys. Rev. Lett.* **93**, 203401–1–203401–4.
- Tadmor, E. B., Ortiz, M. & Phillips, R. (1996) *Philos. Mag. A* **73**, 1529–1563.
- Broughton, J. Q., Abraham, F. F., Bernstein, N. & Kaxiras, E. (1999) *Phys. Rev. B* **60**, 2391–2403.
- Warshel, A. & Levitt, M. (1976) *J. Mol. Biol.* **103**, 227–249.
- Field, M. J., Bash, P. A. & Karplus, M. (1990) *J. Comput. Chem.* **11**, 700–733.
- Barnett, R. N., Cleveland, C. L., Joy, A., Landman, U. & Schuster, G. B. (2001) *Science* **294**, 567–571.
- Perdew, J. P., Burke, K. & Ernzerhof, M. (1996) *Phys. Rev. Lett.* **77**, 3865–3868.
- Kollman, P. A., Dixon, R., Cornell, W., Fox, T., Chipot, C. & Pohorille, A. (1997) *Computer Simulations of Biomolecular Systems* (Elsevier, Amsterdam), Vol. 3.
- Eichinger, M., Tavan, P., Hutter, J. & Parrinello, M. (1999) *J. Chem. Phys.* **110**, 10452–10467.
- Laio, A., VandeVondele, J. & Rothlisberger, U. (2002) *J. Chem. Phys.* **116**, 6941–6947.
- Nielsen, S. O., Lopez, C. F., Srinivas, G. & Klein, M. L. (2004) *J. Phys. Condens. Matter* **16**, R481–R512.
- Voter, F. A., Montalenti, F. & Germann, T. C. (2002) *Annu. Rev. Mater. Res.* **32**, 321–346.